Gels

DOI: 10.1002/anie.201206053

Broad-Spectrum Antimicrobial and Biofilm-Disrupting Hydrogels: Stereocomplex-Driven Supramolecular Assemblies**

Yan Li, Kazuki Fukushima, Daniel J. Coady, Amanda C. Engler, Shaoqiong Liu, Yuan Huang, John S. Cho, Yi Guo, Lloyd S. Miller, Jeremy P. K. Tan, Pui Lai Rachel Ee, Weimin Fan, Yi Yan Yang, and James L. Hedrick**

The development of antibiotic-resistant bacteria has created a myriad of new challenges within the healthcare field. Skin infections caused by drug-resistant *Staphylcoccus aureus* (MRSA) account for more than half of all reported cases of *S. aureus* skin infections in the United States.[1] Furthermore, because of the extremely high occurrence of MRSA infections an estimated 20000 deaths occur annually.[2] Unfortunately, current problems associated with drug-resistant microbes extend far beyond gram-positive bacteria such as MRSA. Perhaps even more distressing is the rapidly increasing antibiotic resistance of gram-negative bacteria, which already suffers from inadequate treatment options.[3] Moreover, bacteria easily colonize the surfaces of tissue, surgical devices (implants, orthopedics, catheters, etc.), and instruments causing more than 85% of surgical device related infections.[4] Bacterial biofilms consist of bacteria and self-secreted extracellular polymeric substances (EPS),[5] and are extremely resistant to conventional antibiotics because of acquired resistance, limited diffusion, and inactivation of antibiotics in EPS.[4,6]

Antimicrobial hydrogels are envisioned to be an integral weapon for combating drug-resistant infections. Since gels exhibit many polymer characteristics without becoming freely dissolved, such materials can remain in place under physiological conditions while maintaining antimicrobial activity. These attributes make them ideal for wound healing, implant/catheter coatings, skin infections, and even orifice-barrier applications. Several antimicrobial hydrogels such as quaternized ammonium chitosan-*graft*-poly(ethylene glycol) methacrylate,[7] epsilon-poly-L-lysine-*graft*-methacrylamide (EPL-MA),[8] polyelectrolyte complexes (PEC),[9] and self-assembled peptides[10] were reported as having broad-spectrum activity. However, most examples are based on chitosan (material derived from crab shells) which can suffer from immunogenicity and material variance, or are produced from expensive peptides. Therefore, there is a pressing need to develop antimicrobial hydrogels from synthetic, cost-effective, and biodegradable materials with well-defined molecular structures. It must also be moldable/processable, thus allowing in situ applications. Furthermore, the antimicrobial hydrogel must remain stable and active for the duration of its purpose. However, upon completion of its intended use it should succumb to natural remediation.

Herein, we describe a simple yet effective approach to generating charged hydrogels using noncovalent interactions, thus overcoming many of the issues plaguing existing antimicrobial hydrogels. More specifically, we report a stimulus-responsive antimicrobial gel formed from stereocomplexation of biodegradable poly(L-lactide)-*b*-poly(ethylene glycol)-*b*-poly(L-lactide) (PLLA-PEG-PLLA) and a charged biodegradable polycarbonate triblock polymer (i.e. PDLA-CPC-PDLA). The stereocomplexes were found to exist as soluble micelles at room temperature in aqueous solution, however, upon heating to physiological temperature (ca. 37 °C) gel-like materials with distinctive supramolecular fiber/ribbon-like structures and shear-thinning behavior were formed. This drastic change in material properties was also accompanied by a significant increase in antimicrobial activity which encompassed gram-positive/gram-negative bacteria, fungi, and microbial biofilms.

In an effort to obtain biodegradable/biocompatible hydrogels free of metal catalyst, all materials were produced using organocatalyzed living ring-opening polymerization (ROP) techniques.[11] The PLLA-PEG-PLLA triblock copolymers synthesized have very narrow molecular weight distributions

[*] Y. Li,[+] Dr. S. Liu, Dr. J. P. K. Tan, Prof. Y. Y. Yang
Institute of Bioengineering and Nanotechnology
31 Biopolis Way, The Nanos, Singapore 138669 (Singapore)
E-mail: yyyang@ibn.a-star.edu.sg
Y. Li,[+] Dr. P. L. R. Ee
Department of Pharmacy, National University of Singapore
18 Science Drive 4, Singapore 117543 (Singapore)
Y. Huang, Dr. W. Fan
Program of Innovative Therapeutics, The First Affiliated Hospital
Zhejiang University College of Medicine, 79 Qingchun Road
Hangzhou 310003 (China)
Dr. J. S. Cho, Dr. Y. Guo, Dr. L. S. Miller
Division of Dermatology, University of California Los Angeles
52-121 Center for Health Sciences, Los Angeles, CA 90095 (USA)
Dr. K. Fukushima[+]
Department of Polymer Science and Engineering
Yamagata University, Yonezawa, Yamagata 992-8510 (Japan)
Dr. D. J. Coady, Dr. A. C. Engler, Dr. J. L. Hedrick
IBM Almaden Research Center
650 Harry Road, San Jose, CA 95120 (USA)
E-mail: hedrick@usa.ibm.com
[+] These authors contributed equally to this work.

[**] This work was funded by the Institute of Bioengineering and Nanotechnology (Biomedical Research Council, Agency, for Science, Technology and Research, Singapore), IBM Almaden Research Center (USA), University of California, Los Angeles (UCLA (USA)), Zhejiang University (China).

Supporting information for this article is available on the WWW under http://dx.doi.org/10.1002/anie.201206053.

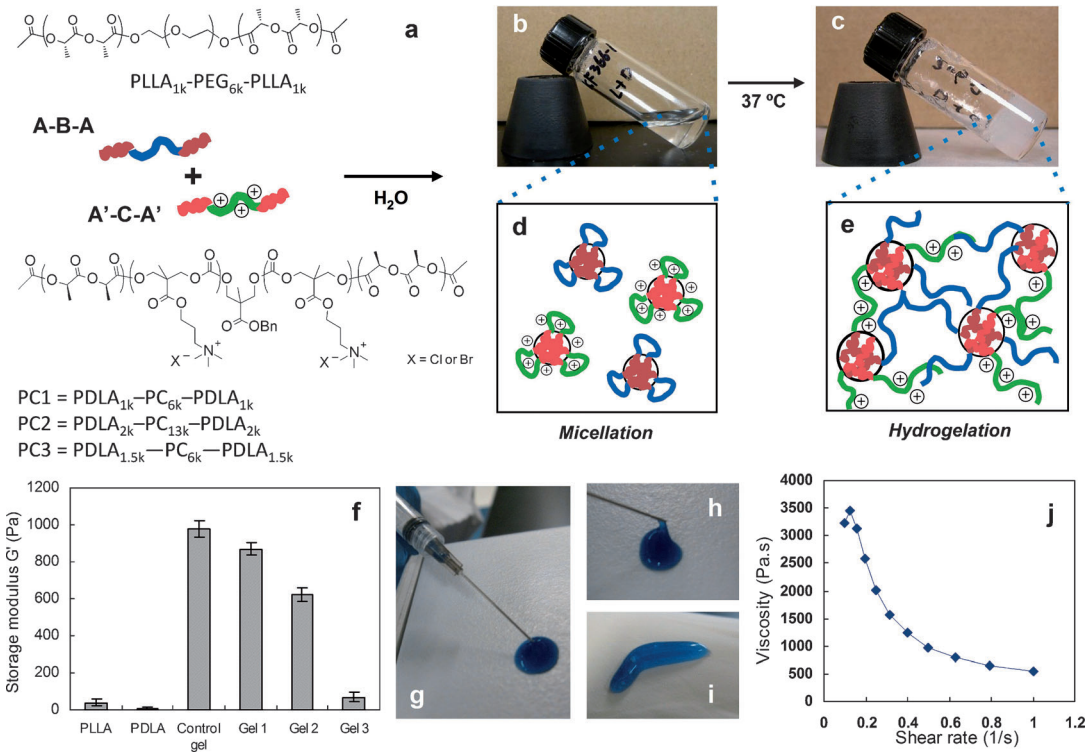

Figure 1. Formulation of mixed micelle solution comprising PLLA-PEG-PLLA and PDLA-CPC-PDLA. Schematic representation (a) and pictures of 10% w/v solution at 25 °C (b) and at 37 °C (c). At 25 °C the solution is clear fluid and each polymer forms flower-type micelles in an aqueous environment (d). Upon heating at 37 °C for 30 min, the solution turns into an opaque gel based on stereocomplex formation between enantiomeric pure polylactide segments in the micelle cores (e). The hydrogel has shear-thinning properties, making it suitable for topical applications as well as for direct injection into various body cavities (f–i), and viscosity as a function of sheer rate (j). Control Gel (PLLA in PLLA-PEG-PLLA and PDLA in PDLA-PEG-PDLA at 1:1 molar ratio), Gel 1 (PLLA in PLLA-PEG-PLLA, PDLA in PDLA-CPC-PDLA, and PDLA in PDLA-PEG-PDLA at 1:0.15:0.85), Gel 2 (1:0.3:0.7 molar ratio), and Gel 3 (PLLA in PLLA-PEG-PLLA and PDLA in PDLA-CPC-PDLA at 1:1 molar ratio).

(Figure 1a). This was accomplished using commercially available PEG diols which served as the central block while concurrently initiating both outer PLA blocks. It was found that PEG polymers of more than 6 kDa allowed complete polymer dissolution in aqueous media assuming lactide blocks remained at or under 1 kDa. Larger hydrophobic blocks could be used but required water-miscible solvents such as tetrahydrofuran (THF) to promote the initial self-assembly of polymers, eventually leading to full water solubility. Analogous triblock polymers were then reproduced using D-lactide (i.e. PDLA-PEG-PDLA) for complementary stereocomplexation studies (Figure 1a). Upon dissolution in water, the PEG-based copolymers, and their mixture having opposite stereochemistries, formed clear solutions (Figure 1b,d). In addition, we observed a cloud point temperature and gelation upon heating the polymer solution above 60 °C (Figure 1c,e). This result corresponded analogously to work reported by Kimura et al.[12] Such behavior is indicative of a lower critical solution temperature (LCST), which was observed for both the enantiomerically pure polymer solutions and stereocomplexed copolymer system (see Figure S1 in the Supporting Information).

Copolymers having shorter PLA block lengths (e.g. Mn = 850 and 1000 g mol^{-1}), required no organic solvent for dispersion in water at ambient temperature. When these solutions were incubated at 37 °C for 5 hours, opaque, low-modulus, and viscous solutions were formed at polymer concentrations of 13.2 % w/v (Figure 1f). Imaging of PLLA-PEG-PLLA with an optical microscope showed an abundance of fiber-like nanostructures, whereas PDLA-PEG-PDLA formed far fewer fiber-like assemblies (see Figure S2 in the Supporting Information). After combining PLLA-PEG-PLLA with PDLA-PEG-PDLA and incubating at 37 °C for 5 h, shorter fibers were formed (Figures S2 and S3) accompanied by gel formation and increased modulus (with respect to enantiomerically pure precursors; Figure 1f). Interestingly, the morphology of stereocomplexes was transformed from micelles into fibers after incubation at 37 °C for 5 hours (see Table S1 in the Supporting Information). This supramolecular gel did not show a melting point associated with the PLA component (Figure S4). A similar finding was reported by Fujiwara and co-workers[13] on annealed samples of di- and triblock copolymers of PLA and PEO. Additionally, O'Reilly and co-workers reported annealed poly(lactide)-*b*-poly(acrylic acid) and poly(lactide)-*b*-poly(dimethylaminoethyl acrylate) micelles which crystallized adjacent lactide blocks that formed high aspect ratio nanostructures.[14]

Functional cationic triblock polymers (PDLA-CPC-PDLA) were constructed by synthesizing a polycarbonate macroinitiator with subsequent D-lactide polymerizations. Following a previously reported procedure,[15] cyclic carbonates with pendent propyl chloride chains were generated

from 2,2-bis(hydroxymethyl)propionic acid [bis(MPA)]. The carbonate monomers were then polymerized from a small-molecule diol, thus affording telechelic polycarbonates.[16] These polymers were then used to initiate D-lactide polymerizations, thereby forming triblock polymers (PDLA-CPC-PDLA) with a well-defined molecular structure. After polymer isolation the pendent propyl chloride chains were quaternized with excess trimethylamine (TMA) in acetonitrile yielding cationic PDLA-CPC-PDLA materials. Three separate PDLA-CPC-PDLA polymer compositions were studied: 1k-6k-1k (PC1), 2k-13k-2k (PC2) and 1.5k-6k-1.5k (PC3). The utilization of a central cationic block produced water-soluble materials, which spontaneously formed spherical micelles ranging from 134 to 181 nm in size with zeta potentials between 25 and 69 mV (see Figure S5 in the Supporting Information). Despite having alkyl ammoniums no antimicrobial activity was observed for PDLA-CPC-PDLA at concentrations below 10000 mg L^{-1} (see Table S2 in the Supporting Information). The cationic triblock polymers were further tested for toxicity against two model mammalian cell types: rat red blood cells and human dermal fibroblasts (HDF). It was found that PC2 was the least toxic among the three copolymers, and no hemolysis was observed for PC2 until about 25000 mg L^{-1} (Figure S6), while maintaining HDF cell viability above 80% (Figure S7).

PDLA-CPC-PDLA (PC2) was then incorporated into PLLA-PEG-PLLA (0.85k-6k-0.85k) and PDLA-PEG-PDLA (1k-6k-1k) gel at different contents by stereocomplexation at 37°C with a total polymer concentration of 13.2% w/v to impart antimicrobial function. Three different gel compositions were studied: Gel 1 (PLLA-PEG-PLLA, PDLA-CPC-PDLA and PDLA-PEG-PDLA at 1:0.15:0.85), Gel 2 (PLLA-PEG-PLLA, PDLA-CPC-PDLA, and PDLA-PEG-PDLA at 1:0.3:0.7), and Gel 3 (PLLA-PEG-PLLA and PDLA-CPC-PDLA at 1:1). The molar ratio of PLLA to PDLA was kept at 1:1 to induce optimal stereocomplexation. Using optical, transmission, and scanning electron microscopies major morphological changes were observed in the gels formed with stoichiometric equivalents of PDLA-CPC-PDLA/PLLA-PEG-PLLA combined (Gel 3), relative to the control gel prepared from PLLA-PEG-PLA/PDLA-PEG-PDLA where fibers could be clearly seen (Figure 2a; and see Figures S8 and S9 in the Supporting Information). Nonetheless, similar to the control gels, a morphological transformation from micelles to fibers was observed when Gel 1 and Gel 2 both having lower amounts of PC2 were formed(see Table S1 in the Supporting Information). Additionally, numerous fibers with similar lengths were seen (Figures S2, S3, and S8). Gel moduli decreased with increasing amounts of PC2 (Figure 1f). This was reasoned to be a result of fiber-like assemblies formed through partial crystallization within the lactide domains.[12] This in turn reinforced the gels manifesting in higher moduli. Furthermore, regardless of PC2 content, moduli was found to increase with longer annealing times, hence supporting the idea of crystalline microdomains (Figure S10). This supposition was also supported by wide-angle X-ray diffraction patterns producing strong signals attributed to the stereocomplex crystallization (Figure 2b). Nonetheless, moduli were relatively low for all three cationic gels (Gel 1, 2, and 3) which is indicative of a noncovalent gel-forming process. As such, the gels were readily remoldable and showed significant drops in viscosity with an increasing shear rate (Figure 1j), thereby providing shear-thinning abilities. This important attribute significantly facilitates deposition through a syringe, thus increasing clinical applicability (Figures 1g–i).

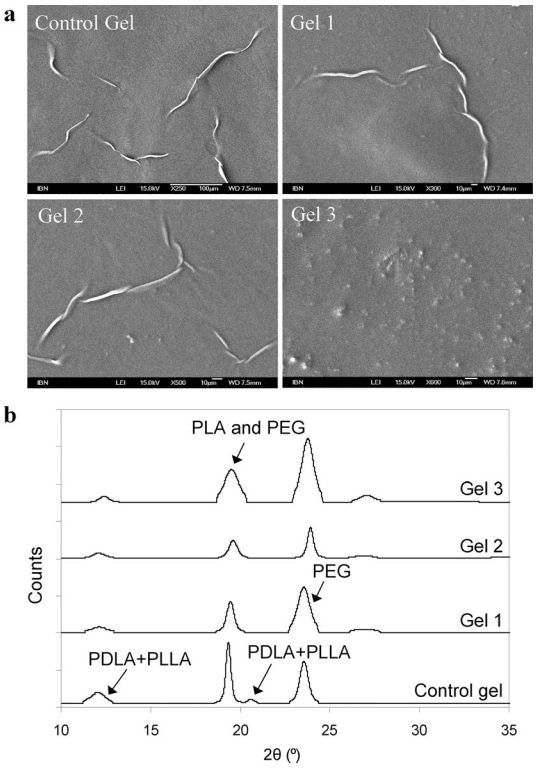

Figure 2. Formation of stereocomplex hydrogels. SEM images (a) and wide-angle X-ray diffraction patterns (b) of Control Gel, Gel 1, Gel 2, and Gel 3. The gels were formed at 13.2% w/v.

Gel antimicrobial activities were evaluated against various pathogenic microbes—*S.* aureus (Gram-positive), *E.* coli (Gram-negative), and *C.* albicans (fungus). At concentrations below 25000 mg L^{-1}, PC2 formed antimicrobial gels without inducing significant hemolysis or cytotoxicity (see Figures S6 and S7 in the Supporting Information). At these concentrations PC2 alone showed no activity (see Table S1 in the Supporting Information). Similarly, the control gel formed from PLLA-PEG-PLLA and PDLA-PEG-PDLA showed no antimicrobial activity (Figure 3). In sharp contrast, the stereocomplex gels made from PLLA-PEG-PLLA, PC2, and PDLA-PEG-PDLA at 1:0.15:0.85 molar ratio (Gel 1, PC2 = 10000 mg L^{-1}) completely suppressed bacterial growth (Figure 3a–c) and killed the bacteria (i.e. *S.* aureus and *E.* coli) with about 100% efficiency (Figure S11). A gel with an increased amount of PC2 (Gel 2, 20000 mg L^{-1}) was needed to inhibit *C.* albicans growth and completely eliminate the fungus (Figure S11).

To demonstrate clinical potential the antimicrobial gels were tested against clinically isolated microbes—methicillin-resistant *S.* aureus (MRSA, gram-positive), vancomycin-resistant enterococci (VRE, gram-positive), *P.* aeruginosa

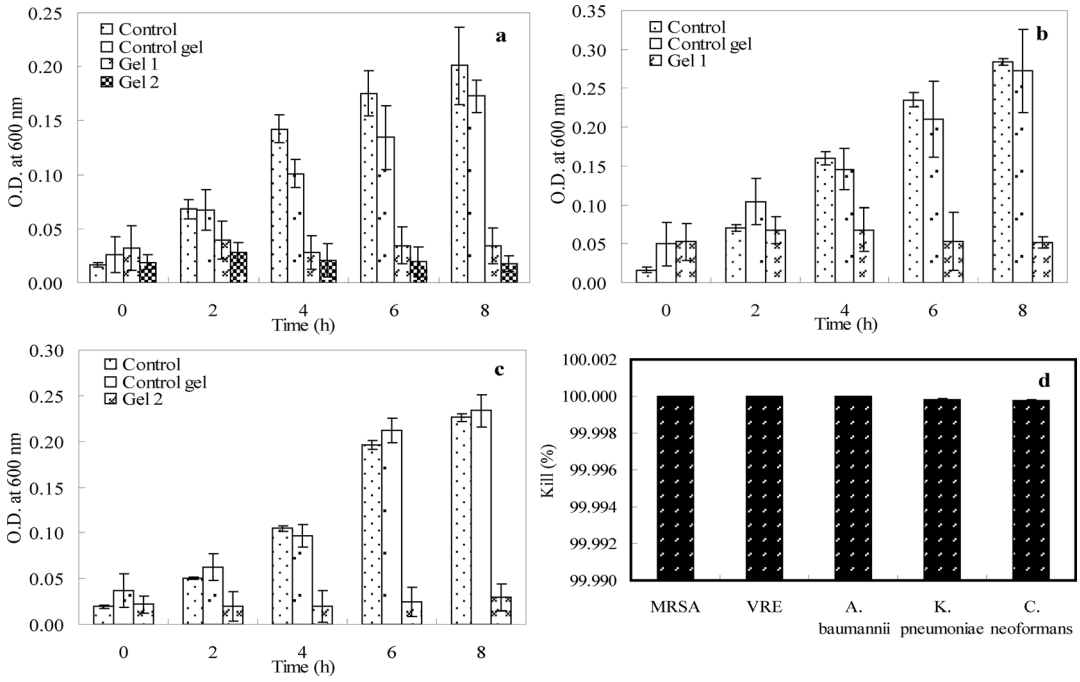

Figure 3. Antimicrobial activities of cationic hydrogels against various microbes. Growth inhibition of *S.* aureus (gram-positive; a), *E.* coli (gram-negative; b), and *C.* albicans (fungi; c). Shown is the % killing efficiency of various clinically isolated multidrug-resistant microbes by using Gel 1 (d).

(gram-negative), *A.* baumannii (gram-negative, resistant to most antibiotics), *K.* pneumoniae (gram-negative, resistant to carbapenem), and *C.* neoformans. The gels were found to completely inhibit growth and showed a nearly perfect killing efficiency on all microbial cells tested (Figure 3d).

The mechanism of antimicrobial action was determined to be cell wall/membrane lysis. This conclusion was supported by morphological changes of *S.* aureus, *E.* coli, and *C.* albicans after incubation with the antimicrobial gels for two hours. Shown in Figure 4, untreated microbial cells and cells treated with the control gel remained smooth and in their respective round (*S.* aureus and *C.* albicans) or rodlike (*E.* coli) shape. In sharp contrast, cellular deformation and surface roughness were clearly seen after exposure to an antimicrobial gel. Additionally, lysed cells and debris were also observed in treated microbe samples. In the case of *E.* coli, numerous vesicle-like structures were formed, presumably from gel–cell membrane integration (white arrows in Figure 4b). Further supporting a catastrophic membrane failure mechanism was the observation of released cytoplasts from *C.* albicans upon gel exposure (Figure 4c).

The ability of the gels to disperse biofilms was tested against *S.* aureus, MRSA, *E.* coli, and *C.* albicans. After gel exposure, more than 60% of film biomass had been removed, and nearly 80% of bacterial cells killed with only a single treat-

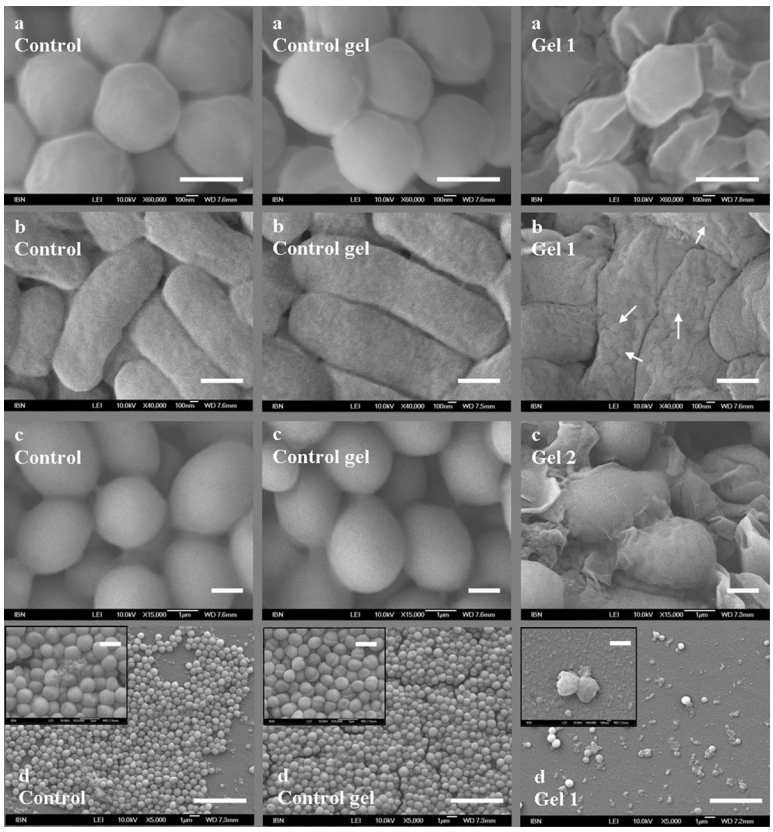

Figure 4. SEM images of *S.* aureus (a), *E.* coli (b), *C.* albicans (c), and MRSA biofilm (d) before (Control) and after incubation with Control Gel, Gel 1 (*S.* aureus, *E.* coli and MRSA), and Gel 2 (*C.* albicans) for 2 h (biofilm: 24 h). Scale bar for a, b: 500 nm; c: 1 μm; d: 5 μm. Scale bar for Control and Control Gel samples (insert): 1 μm; Gel 1 sample (insert): 500 nm.

ment (see Figure S12 in the Supporting Information). Biofilm dispersion was further evaluated by the SEM before and after treatment (Figure 4d; and see Figures S13 and S14). To the best of our knowledge this type of biofilm disruption has not been reported in other antimicrobial hydrogels/synthetic polymers.

The safety of antimicrobial hydrogels was evaluated for skin sensitization, acute dermal toxicity, and skin irritation. These studies were performed using rats, guinea pigs, and rabbits at good lab practice (GLP) facilities and according to international regulatory guidelines (see the Supporting Information). No adverse effects (skin sensitization, dermal toxicity, or irritation) were observed. Additionally, the hydrogel LD50 value was greater than 2000 $mg\,kg^{-1}$, thereby demonstrating clinical feasibility in topical applications.

In conclusion, the use of lactide stereocomplexation provided a thermally sensitive means for producing supramolecular antimicrobial hydrogels. Because of the nature of their noncovalent associations, these materials were shown to exhibit shear-thinning properties. Moreover, the hydrogels induced no significant hemolysis or cytotoxicity towards mammalian cells, and demonstrated excellent skin biocompatibility. The combination of broad-spectrum antimicrobial activity (encompassing multidrug-resistant Gram-positive/negative bacteria, fungi, and biofilm) with moldable/processable capabilities makes these nontoxic materials ideal for injectable, topical, and coating applications.

Received: July 28, 2012
Revised: October 1, 2012
Published online: November 19, 2012

Keywords: biofilms · gels · electron microscopy · noncovalent interactions · supramolecular chemistry

[1] Methicillin-Resistant Staphylococcus Aureus (MRSA)", can be found under http://www.cdph.ca.gov/healthinfo/discond/Pages/MRSA.aspx (**2010**).
[2] G. Taubes, *Science* **2008**, *321*, 356 – 361.
[3] J. Davies, D. Davies, *Microbiol. Mol. Biol. Rev.* **2010**, *74*, 417 – 433.
[4] J. W. Costerton, L. Montanaro, C. R. Arciola, *Int. J. Artif. Organs* **2007**, *30*, 757 – 763.
[5] P. Watnick, R. Kolter, *J. Bacteriol.* **2000**, *182*, 2675 – 2679.
[6] a) K. Lewis, *Curr. Top. Microbiol. Immunol.* **2008**, *322*, 107 – 131; b) R. Kharidia, J. F. Liang, *J. Microbiol.* **2011**, *49*, 663 – 668.
[7] P. Li, Y. F. Poon, W. Li, H. Y. Zhu, S. H. Yeap, Y. Cao, X. Qi, C. Zhou, M. Lamrani, R. W. Beuerman, E. T. Kang, Y. Mu, C. M. Li, M. W. Chang, S. S. Leong, M. B. Chan-Park, *Nat. Mater.* **2011**, *10*, 149 – 156.
[8] C. Zhou, P. Li, X. Qi, A. R. Sharif, Y. F. Poon, Y. Cao, M. W. Chang, S. S. Leong, M. B. Chan-Park, *Biomaterials* **2011**, *32*, 2704 – 2712.
[9] C. T. Tsao, C. H. Chang, Y. Y. Lin, M. F. Wu, J. L. Wang, J. L. Han, K. H. Hsieh, *Carbohydr. Res.* **2010**, *345*, 1774 – 1780.
[10] D. A. Salick, J. K. Kretsinger, D. J. Pochan, J. P. Schneider, *J. Am. Chem. Soc.* **2007**, *129*, 14793 – 14799.
[11] a) N. E. Kamber, W. Jeong, R. M. Waymouth, R. C. Pratt, B. G. G. Lohmeijer, J. L. Hedrick, *Chem. Rev.* **2007**, *107*, 5813 – 5840; b) S. H. Kim, J. P. K. Tan, F. Nederberg, K. Fukushima, Y. Y. Yang, R. M. Waymouth, J. L. Hedrick, *Macromolecules* **2008**, *42*, 25 – 29; c) F. Nederberg, B. G. G. Lohmeijer, F. Leibfarth, R. C. Pratt, J. Choi, A. P. Dove, R. M. Waymouth, J. L. Hedrick, *Biomacromolecules* **2006**, *8*, 153 – 160; d) R. C. Pratt, B. G. G. Lohmeijer, D. A. Long, P. N. P. Lundberg, A. P. Dove, H. Li, C. G. Wade, R. M. Waymouth, J. L. Hedrick, *Macromolecules* **2006**, *39*, 7863 – 7871.
[12] a) T. Fujiwara, T. Mukose, T. Yamaoka, H. Yamane, S. Sakurai, Y. Kimura, *Macromol. Biosci.* **2001**, *1*, 204 – 208; b) T. Mukose, T. Fujiwara, J. Nakano, I. Taniguchi, M. Miyamoto, Y. Kimura, I. Teraoka, C. Woo Lee, *Macromol. Biosci.* **2004**, *4*, 361 – 367.
[13] a) T. Fujiwara, M. Miyamoto, Y. Kimura, T. Iwata, Y. Doi, *Macromolecules* **2001**, *34*, 4043 – 4050; b) T. Fujiwara, M. Miyamoto, Y. Kimura, *Macromolecules* **2000**, *33*, 2782 – 2785; c) D. G. Abebe, T. Fujiwara in *240th ACS National Meeting, Vol. 51*, American Chemical Society, Boston, MA, **2010**, p. 409.
[14] N. Petzetakis, A. P. Dove, R. K. O'Reilly, *Chem. Sci.* **2011**, *2*, 955 – 960.
[15] D. P. Sanders, K. Fukushima, D. J. Coady, A. Nelson, M. Fujiwara, M. Yasumoto, J. L. Hedrick, *J. Am. Chem. Soc.* **2010**, *132*, 14724 – 14726.
[16] F. Nederberg, Y. Zhang, J. P. K. Tan, K. Xu, H. Wang, C. Yang, S. Gao, X. D. Guo, K. Fukushima, L. J. Li, J. L. Hedrick, Y. Y. Yang, *Nat. Chem.* **2011**, *3*, 409 – 414.

